Available online at www.sciencedirect.com
ScienceDirect
Journal of Photochemistry and Photobiology A: Chemistry 187 (2007) 339–347
Journal of Photochemistry and Photobiology A:Chemistry
www.elsevier.com/locate/jphotochem

Assessment of solvent effect on the relaxation dynamics of milrinone

Maged El-Kemary [1], Juan Angel Organero, Abderrazzak Douhal *

Departamento de Química Física, ICAM and Sección de Químicas, Facultad de Ciencias del Medio Ambiente, Universidad de Castilla-La Mancha, Avda. Carlos III, S.N., 45071 Toledo, Spain

Received 13 June 2006; received in revised form 30 October 2006; accepted 31 October 2006
Available online 7 November 2006

Abstract

We report a study of the effect of solvent properties (polarity, H-bonding and viscosity) on the relaxation dynamics of milrinone (MIR) by using steady-state UV–vis absorption, emission and picosecond emission techniques. The major solvent effect on the steady-state absorption and emission spectra is due to specific interactions between solvent molecules and different sites of MIR, although the effect of medium polarity is not negligible. Time-resolved experiments provided more information. The observed effect on the relaxation dynamics is due to H-bonding acceptor ability, polarity and viscosity of the solvent. The result is explained in terms of the presence of an intramolecular charge-transfer reaction and twisting motion. The anisotropy decay data suggest that MIR rotates under stick boundary conditions. We believe that these results might be of importance for improving drugs design and may help to understand the interactions of MIR and other drugs with the environment.

Keywords: Milrinone; Pyridone; Drug; Cardiotonic; Dynamics; Relaxation; Twisting; Hydrogen bonding; Lifetime; Anisotropy; Emission

1. Introduction

Milrinone (scheme, MIR), 1,6-dihydro-2-methyl-6-oxo-3,4′-bipyridine-5-carbonitrile, a cardiotonic drug, is an inotropic agent used for the short term intravenous therapy of congestive heart failure [1]. This drug can exist in different tautomeric and conformational structures in the ground and excited states [2–4]. The electron donating methyl substitutent of MIR drives the equilibrium towards the keto form in water [3,5,6]. Theoretical calculations predict ~7 kcal/mol energy gap between the keto and enol forms, the former one being the more stable structure [4]. From the point of view of medical use, both keto and cation structures are the active forms [2,7].

The short time of action of MIR is promising. However, long-term of use the oral form of the drug revealed that it is associated with adverse side effects [8–11]. Detailed knowledge about solvent interactions with drug at the S_0 and S_1 states is essential for drug design and synthesis, and for the evaluation of photostability and phototoxicity of the drug. Therefore, the involved molecular mechanism can be explored through the study of the fast dynamic aspects of the drug photorelaxation in different media [12–14]. The H-bonding, twisting motion and intramolecular charge transfer (ICT) are perhaps key features for inotropic activity of keto (K) and cation structures [4]. An assessment of the solvent effect on its photodynamics may help for a better understanding of its interactions with the environment (for example water and biological molecules—its target protein and/or membrane transport). Such a result may also help to understand the behavior of other medicines having comparable groups.

Therefore, the information may add new knowledge to improve drugs design and use in phototherapy where the outcome of the interaction of light with the medicine is of great importance. In previous studies, we have reported on the fast dynamics of MIR in water and in cyclodextrin nanocavities [4,15]. We also showed that in neutral water solutions, K form undergoes an ICT reaction at S_1 in a time constant shorter than 100 fs, followed by a 10-ps dynamics assigned to vibrational relaxation/cooling and twisting motion in the formed ICT state [16]. Here, we report on the fast dynamics of excited MIR, in solvents of various polarity, viscosity and H-bonding ability to

* Corresponding author. Fax: +34 925 268840.
E-mail addresses: elkemary@yahoo.com (M. El-Kemary), Abderrazzak.douhal@uclm.es (A. Douhal).
[1] Present address: Department of Chemistry, Faculty of Science, Kafr ElSheikh University, 33516 Kafr ElSheikh, Egypt.

1010-6030/$ – see front matter © 2006 Elsevier B.V. All rights reserved.
doi:10.1016/j.jphotochem.2006.10.032

gain more insight into the drug–solvent interaction. The results show the importance of H-bonding, ICT and twisting motion on the photorelaxation of the drug.

2. Experimental

MIR (purity ≥ 97%), purchased from Sigma–Aldrich was used as received. Its purity was checked by thin layer chromatography (TLC). Solvents (spectroscopic grade, purchased from Sigma–Aldrich or Merck) were dried and distilled when necessary before use. Steady-state absorption and emission spectra were recorded on Varian (Cary E1) and Perkin-Elmer (LS 50B) spectrophotometers, respectively. Fluorescence quantum yields were determined using quinine sulphate in 0.1N H_2SO_4 as a standard [17]. Emission decays were measured by a time-correlated single photon counting system described before [18]. The sample was excited by a 40 ps pulsed (20 MHz) laser centered at 371 nm and the emission signal was collected at the magic angle. The instrumental response function (IRF) of the apparatus was typically 65 ps. Multiexponential functions convoluted with the IRF signal were fitted to the emission decays using the Fluofit package. The quality of the fits was characterized in terms of residual distribution and reduced χ^2 value. All the measurements were done at 293 ± 1 K.

3. Results and discussion

3.1. Steady-state absorption and fluorescence spectra

In a previous study, we observed that the keto (K) form is the dominant species of MIR in neutral water solution [4]. Like in the case of parent unsubstituted pyridone [19], no indication of phototautomerization was found in solution [4], though this photoreaction is normally observed in heteroaromatic compounds [20–22].

Results of X-ray crystallography (solid state), ^{1}H NMR studies (water solution) and theoretical calculations (gas phase) showed that K is stable under a rotameric conformation in which the pyridone part is rotated by 52° around the C–C bond connecting the two aromatic moieties [4,23].

The UV–vis absorption and fluorescence spectra of MIR were measured in different solvents. Fig. 1 shows representative spectra. Table 1 lists the absorption and fluorescence data together with some solvent parameters [24–26]. The steady-state results indicate a relatively small solvent effect on the absorption and fluorescence maxima reflected in position and shape of the bands. The absorption maxima of MIR in the studied solvents are observed at 340–350 nm ($S_0 \rightarrow S_1$ transition) and 265–275 nm ($S_0 \rightarrow S_2$ transition), whereas the emission maxima are located

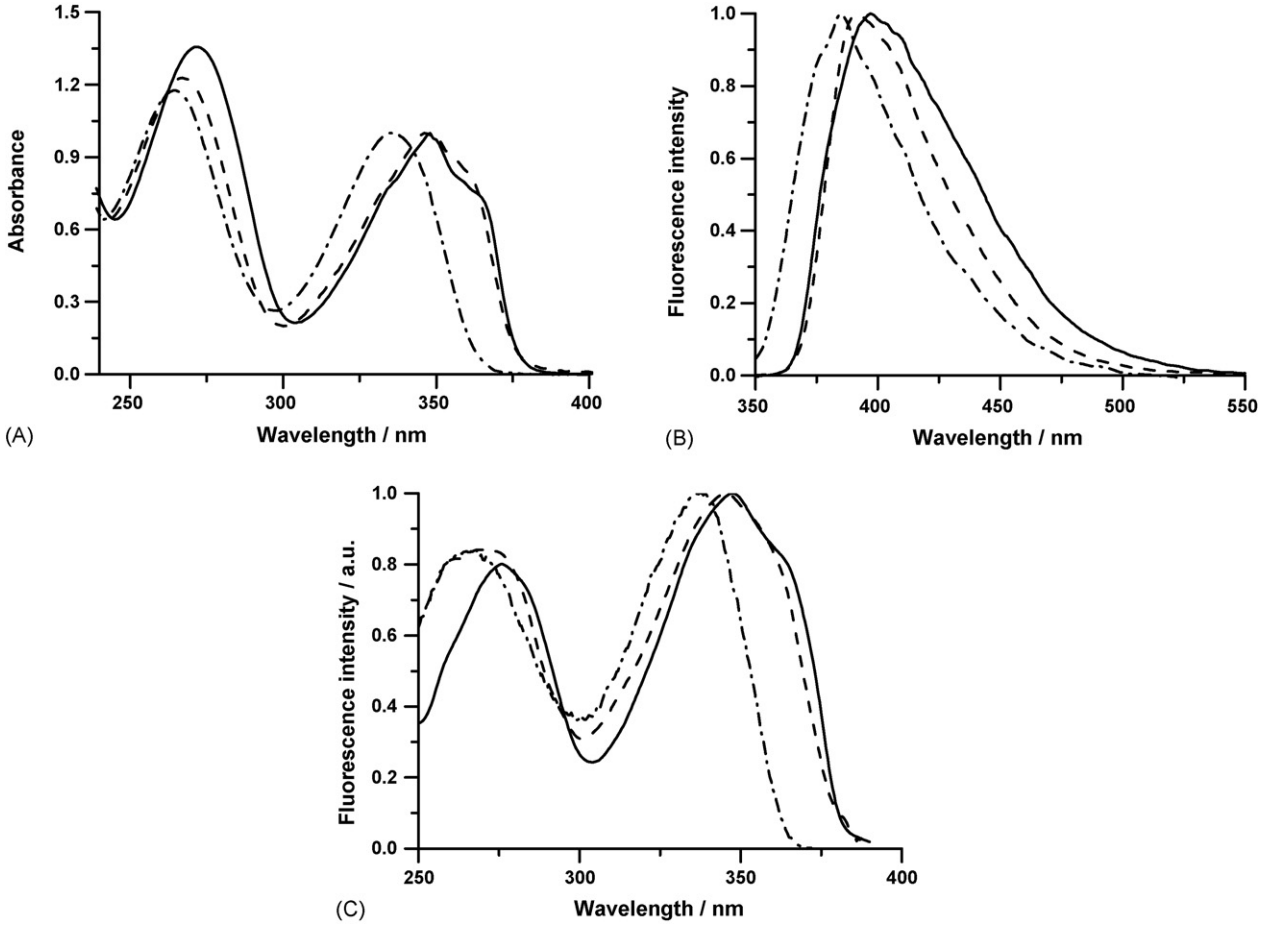

Fig. 1. (A) UV–vis absorption, and (B) emission spectra of MIR in 1,4-dioxane (—), acetonitrile (- - -) and water (– –) solutions. (C) Excitation spectra of MIR in 1,4-dioxane (—), acetonitrile (- - -) and water (– –) observed at 390 nm. For the emission spectra, the excitation wavelength was 340 nm.

Table 1
Steady-state UV–vis absorption and fluorescence data of MIR in different solvents at maximum intensity

	Solvent	λ_a (nm)	λ_f (nm)	$\Delta\tilde{\nu}$ (cm^{-1})	$f(\varepsilon,n)$	η (cP)	E_T (30)	α	β	π^*
1	1,4-Dioxane	266, 348	397	3546	0.03	1.42	36.0	0	0.37	0.49
2	Diethyl ether	268, 350	397	3383	0.30	0.23	34.5	0	0.47	0.24
3	THF	268, 350	394	3190	0.44	0.46	37.4	0	0.55	0.55
4	CH_2Cl_2	265, 347	393	3373	0.47	0.40	40.7	0.13	0.00	0.73
5	DMSO	274, 350	395	3254	0.66	1.99	45.1	0	0.76	1.00
6	CH_3OH	270, 341	390	3685	0.71	0.55	55.5	0.98	0.66	0.60
7	Ethylene glycol	260, 339	397	4310	0.67	20.8	53.8	0.90	0.52	0.92
8	CH_3CN	267, 346	392	3392	0.71	0.37	45.6	0.19	0.31	0.66
9	Water	266, 334	385	3966	0.76	1.00	63.1	1.17	0.47	1.09

This table also contains solvent parameters (see text for detail).

at 392–400 nm. These values are not far from those observed in neutral water: 334, 266 and 385 nm, respectively, suggesting that K is the dominant structure in these media. The spectral band positions of MIR are shifted to longer wavelengths when compared to those reported for pyridone derivatives not having CN, CH_3 and pyridyl groups [27]. Note that for MIR, the CH_3 group may interact with the π system of the pyridone ring through an hyperconjugation stabilizing its rotamer at the excited state, as it has been reported for 1-methyl-2(1H)-pyridone in which the methyl is rotated by 60° with respect to that of the ground state [28]. Ground-state theoretical calculations for K of MIR and of 5-methyl-3,4′-bipyridin-6(1H)-one (MB, a structure similar to MIR but without the CN group) reveal that within a water cavity (continuum dielectric model), the dipole moment value of MB (4.1 D) is lower than that of MIR (10.5 D), revealing that the CN group significantly induces a charge redistribution at the ground state of MIR. Moreover, for MIR the calculations indicate that the Mulliken charge density is −0.828 a.u. at the CN group and +0.877 a.u. at the rest of pyridone moiety [4]. This charge difference shows that an electronic flow at S_0 takes place from the pyridone part to the CN group. The fluorescence excitation spectra (Fig. 1C) in aprotic nonpolar (1,4-dioxane), protic polar (water) and aprotic polar (acetonitrile) solvents are almost similar to those of the absorption ones, except that the relative intensity of the S_2 transition band to that of S_1 is slightly smaller when compared to that in the absorption spectra. The small difference might be due to more efficient non-radiative channel at higher energy of excitation.

An analysis of the solvatochromic shift of absorption and emission bands revealed that the wavelengths of absorption and emission maxima are shifted to shorter values when increasing polarity and H-bonding ability of the solvent (Table 1). This trend is consistent with that reported for comparable pyridone molecules [27]. In water and methanol solutions, the observed blue shift is due to the presence of H-bonding complexes in which both N–H and C=O groups of K are associated with solvent molecules, probably forming a cyclic complex as in the case of 2-pyridone (2PY) [29]. The interaction with the C=O group provokes a decrease in the electronic delocalization of the electrons lone-pair to the pyridone π system and therefore a blue shift in the absorption spectrum. Furthermore, a larger H-bonding energy in the ground state than in the excited one can also lead to the same effect, and will contribute to a blue shift of the spectra. The complexation of 2-PY with water produces a blue shift in the electronic origins relative to the uncomplexed molecule, and the experimental result was explained in terms of a stronger intermolecular H-bond between both molecules at the ground state than in the excited one [30]. Note that for 1,4-dioxane and diethyl ether, the solvent molecule can only bind to the N–H proton of MIR. To analyze the solvent effect on the ground and excited states, we examined the variation of $\tilde{\nu}_{abs}$, $\tilde{\nu}_{em}$ and $\Delta\tilde{\nu}$ ($\tilde{\nu}_{abs} - \tilde{\nu}_{em}$ = Stokes shift) with some solvent characteristics. Table 1 displays the related parameter values.

Fig. 2A shows the variation of $\tilde{\nu}_{abs}$ and $\tilde{\nu}_{em}$ with the value of E_T (30) [24]. While the sensitivity of these transitions to this solvent parameter, governed by polarity and H-bonding acidity of the solvent, is not large, the best correlation is obtained for the change of the absorption transition with a correlation coefficient $R = 0.92$ (Eq. (1)). For emission transition, we got $R = 0.74$ and S.D. = 188. If we use the reaction dielectric field factor to analyze the change ($f(\varepsilon,n) = [(\varepsilon - 1)/(\varepsilon + 2)] - [(n^2 - 1)/(n^2 + 2)]$), where ε and n are the dielectric constant and the refractive index of the solvent, respectively), we obtained a very weak $R \sim 0.6$ for the absorption and emission transitions. When the analysis is performed in terms of Kamlet–Abboud–Taft solvent parameters: H-bond donating acidity (α), H-bond accepting basicity (β) and polarity/polarizability (π^*) [25], the correlation for $\tilde{\nu}_{em}$ is very weak ($R = 0.68$ and S.D. = 240), while that for $\tilde{\nu}_{abs}$ gives 0.97 (Eq. (2)).

$$\tilde{\nu}_{abs}(cm^{-1}) = 26774 + 48E_T(30),$$
$$R = 0.923, \quad \text{standard deviation (S.D.)} = 211 \tag{1}$$

$$\tilde{\nu}_{abs}(cm^{-1}) = 28636 + 920\alpha - 351\beta + 246\pi^*,$$
$$R = 0.967, \quad \text{S.D.} = 112 \tag{2}$$

Therefore, from the above analysis of the absorption and emission transitions position when changing the solvent nature, we can conclude the following: the spectral position of the emission band is relatively less sensitive and shows a lower correlation with the variation of the used solvent parameters, when compared to the absorption one. For this transition, taking into account the characteristics of the used parameters in Eqs. (1) and (2), an increase in the polarity and acidity of the medium shifts the absorption band to shorter wavelengths, while the reverse

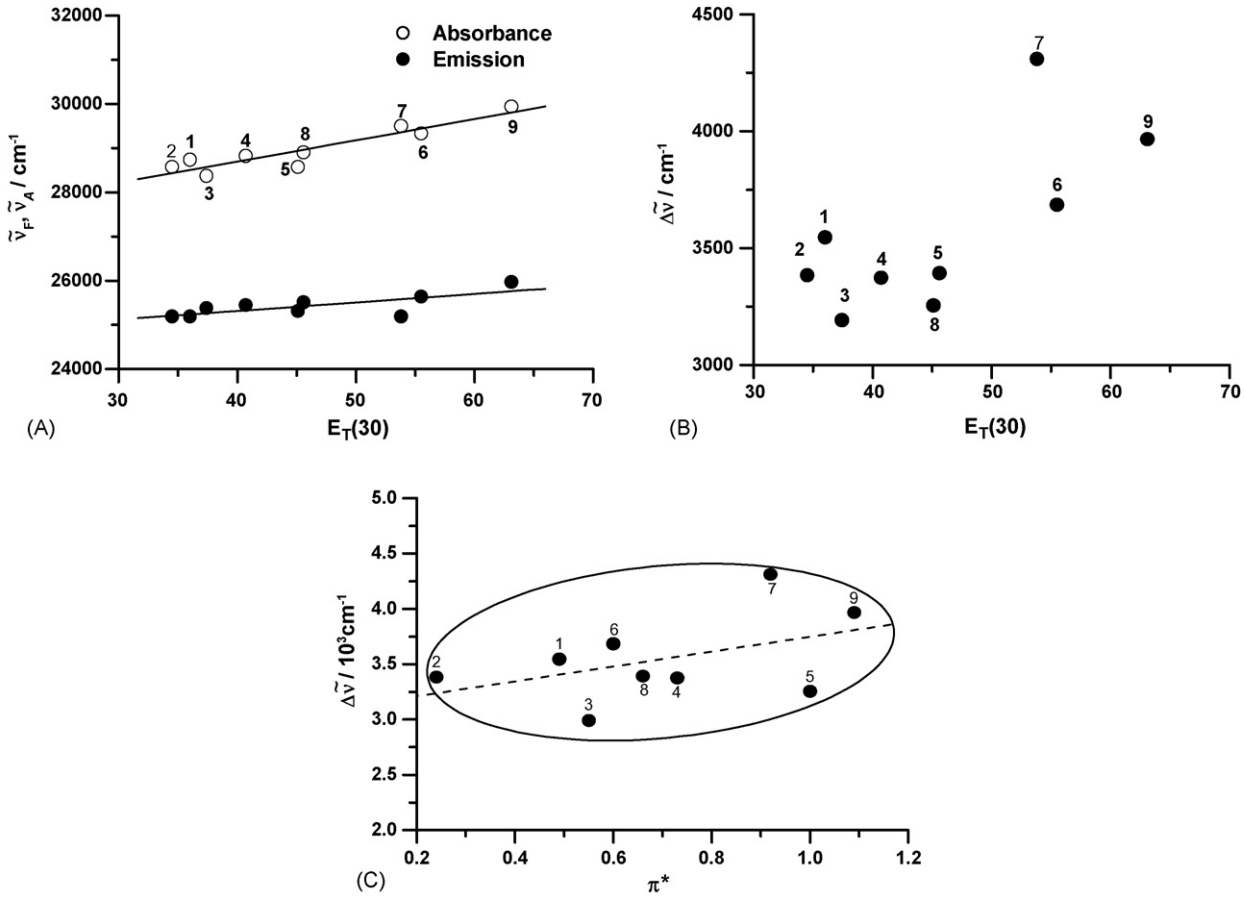

Fig. 2. (A) Variation of $\tilde{\nu}_F$ (●) and $\tilde{\nu}_A$ (○) with E_T (30), (B) variation of Stokes shift ($\Delta\tilde{\nu}$) vs. E_T (30), and (C) variation of $\Delta\tilde{\nu}$ vs. π^*. The dashed line is only to guide the eye and the circle is to envelope the trend. The solvent parameters and numbers are listed in Table 1 (see text for detail).

is obtained when the basicity of the medium increases. The improvement of the correlation, reflected in the values of R and S.D. in Eqs. (1) and (2), shows that the basicity of solvent through H-bond donating ability (reflected in β) affects the spectral position of S_1 transition. The value of coefficients in Eq. (2) shows the acidity of the solvent (α) has the largest effect, while its polarity–polarisability (π^*) exhibits the lowest one.

We analyzed the variation of $\Delta\tilde{\nu}$ with the above solvent parameters, and we observed low and dispersed sensitivity of the $\Delta\tilde{\nu}$ to $f(\varepsilon,n)$ (not shown), E_T (30) and π^* scales (Fig. 2B and C). Therefore, we analyzed the $\Delta\tilde{\nu}$ value change in terms of α, β and π^*, and we obtained:

$$\Delta\tilde{\nu}(\text{cm}^{-1}) = 3373 + 620\alpha - 151\beta + 42\pi^*,$$
$$R = 0.700, \quad \text{S.D.} = 253 \qquad (3)$$

To begin with, the quality of the correlation, the value of R is not good, and that of S.D. is high. Both values reflect a significant deviation of the related points from the expected fit. The scattering of the data is probably because MIR is a multifunctional molecule with possible different kinds of interactions with the solvent (Scheme 1). Four sites of MIR are sensitive to H-bonding interactions with the medium: C=O, NH, C≡N groups, as well as the nitrogen atom of 3-(4-pyridyl) moiety; and two possible ICT reactions in the first electronically excited state may happen: one from the pyridone part to the CN group and the pyridone to pyridyl moieties, as well as twisting motion [4]. The interaction with the solvent will influence the extent of these intramolecular events happening at the excited state, and therefore on the emission quantum yield and spectral position of the remaining emission.

The positive sign of α and π^* coefficients in Eq. (3) indicates that the H-bond donor (HBD) acidity and polarity/polarizability of the solvent lead to an increase in the Stokes shift values of MIR when the value of these solvent parameters increases. The extent of the relative contribution is larger for α (normalized coefficient: 76%) than for π^* (5%). The negative coefficient of

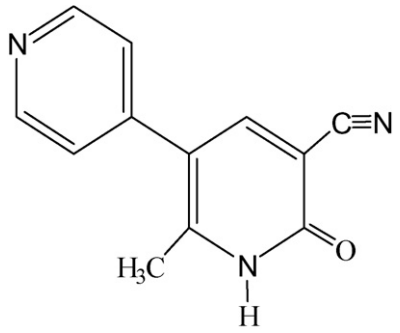

Scheme 1. Molecular structure of keto form of MIR.

β (−151) indicates the reverse trend: an increase of the basicity through HBA ability leads to a lower value of $\Delta\tilde{\nu}$. The larger coefficient for α relative to that of β suggests that the HBD acidity of solvent has more effect on the spectral behavior of MIR compared to the H-bond acceptor (HBA) basicity. Therefore, in the push–pull H-bonding interactions of MIR with the solvent, the acidity of the medium has the stronger effect on $\Delta\tilde{\nu}$ and the resulted electronic flow balance should affect the ICT reactions (from the pyridone part to the CN group or to the pyridyl moiety) at S_1. Both polarity and H-bonding ability of the solvent have been accounted for complicated medium effects on UV absorption and fluorescence emission spectra of pyridone derivatives [31]. For MIR, the $S_1(\pi,\pi^*)$ state of K may be easily mixed with the close lying $S_2(n,\pi^*)$ state through a vibronic coupling, and the extent of this coupling should be sensitive to the polarity and H-bond donating ability of the solvent. For 2-pyridone, complexation with water shifts the 0–0 transition to the blue, a result which indicates a weaker H-bond formed between the S_1 state and water than with the S_0 state and water [30]. Thus, the relative position (energy) of $S_1(\pi,\pi^*)$ state to that of $S_2(n,\pi^*)$ one should be sensitive to H-bonding acidity (α) of the solvent, and Eq. (3) predicts that an increase in α induces an increase in $\Delta\tilde{\nu}$ for which the main involved transitions are of (π,π^*) type. An increases in the acidity of the solvent stabilizes more the S_0 state than the excited $S_1(\pi,\pi^*)$ one, but it destabilizes the S_2 (n,π^*) state, and therefore leads to a larger energy gap between $S_1(\pi,\pi^*)$ and $S_2(n,\pi^*)$ and to a lower vibronic coupling. A stronger coupling induces a faster non-radiative deactivation of the S_1 state. On the other hand, any molecular distortion or twisting motion will affect the above coupling and the electronic conjugation within MIR. As said previously, the methyl group may rotate and interact with the π system of the pyridone ring (hyper conjugation), and the pyridyl moiety shows a twisting motion [4,15].

3.2. Picosecond time-resolved emission study

For a better understanding of the interactions of MIR with the used solvents, we recorded the emission decays upon excitation at 371 nm. Representative ps-emission decays observed at 440 nm in 1,4-dioxane and dimethyl sulfoxide (DMSO) are shown in Fig. 3. Table 2 presents the data of the multi-exponential fits and the values of fluorescence quantum yield (Φ_f) together with those of the radiative (k_r) and non-radiative (k_{nr}) rate constants in various solvents. The results clearly indicate that the excited-state photorelaxation of MIR is sensitive to the solvent properties. For less polar and aprotic media, Φ_f is around 3×10^{-3} and the emission lifetimes (τ) are in the range of 25–45 ps, respectively. For polar and H-bonding acceptor solvents, both Φ_f and τ significantly increase (Table 2). In addition to this change in these solvents, a 0.5–2 ns lifetime appears in the emission decays with weak amplitude (1–3%). The major picosecond component having lifetime in the range 25–270 ps (97–99%) is assigned to the excited keto form of MIR according to a previous report in water [4]. The minor component might be due to a formed and relaxed ICT state [4,15], as it was previously shown in water solutions, or due to a zwitterionic structure of MIR. Because of the limited ps-time resolution of the used apparatus (∼10 ps after deconvolution of the signal using and IRF of 65 ps), we could not observe any rising ps-component in the emission decay of ICT state. Femtosecond transients of MIR in neutral water showed an ultrafast component having a time shorter than 100 fs, and assigned to an ICT reaction of excited K in water solution [16].

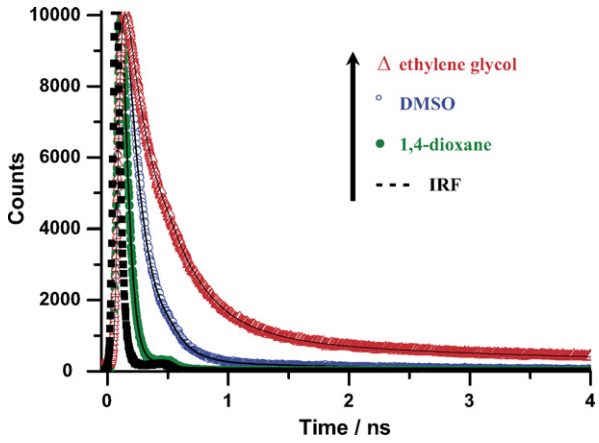

Fig. 3. Magic-angle emission decays of MIR in different solvents gated at 440 nm and upon excitation at 371 nm. The data of the multi-exponential fits (solid lines) are shown in Table 2. The figure shows the IRF (65 ps) of the apparatus.

Table 2
Values of fluorescence quantum yield (Φ_f), emission lifetime (τ_i), and normalized (to 100) pre-exponential factor (a_i) of fitting decay function in different solvents

	Solvent	Φ_f	τ_1 (ps)	a_1 (%)	τ_2 (ns)	a_2 (%)	k_r[a] (10^8 s^{-1})	k_{nr}[b] (10^9 s^{-1})
1	1,4-Dioxane	0.004	45	100			0.9 ± 0.2	22 ± 4
2	Diethyl ether	0.003	24	100			1.2 ± 0.2	41 ± 8
3	THF	0.005	39	99	0.95	1	1.3 ± 0.3	25 ± 5
4	CH_2Cl_2	0.003	24	100			1.2 ± 0.2	41 ± 8
5	DMSO	0.067	135	98	2.0	2	4.9 ± 0.4	7 ± 2
6	CH_3OH	0.010	50	97	0.5	3	2.0 ± 0.4	20 ± 4
7	Ethylene glycol	0.033	270	99	1.9	1	1.2 ± 0.3	3.6 ± 1
8	CH_3CN	0.005	29	99	1.5	1	1.7 ± 0.4	34 ± 6
9	Water	0.014	65	99	1.34	1	2.1 ± 0.4	15 ± 3

k_r and k_{nr} are the radiative and non-radiative rate constants, respectively.
[a] $k_r = \Phi_f/\tau_1$.
[b] $k_{nr} = (1 - \Phi_f)/\tau_1$.

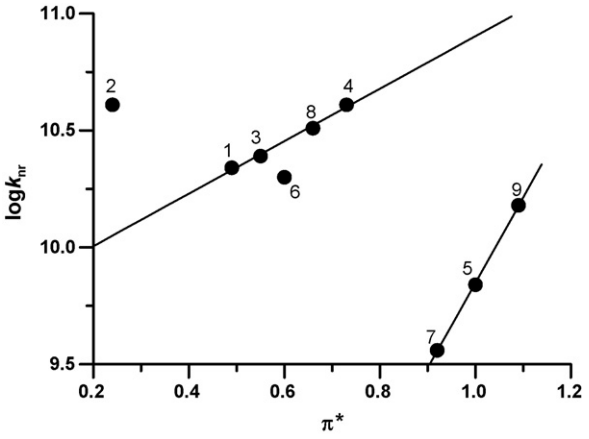

Fig. 4. Plot of log k_{nr} vs. π^*. The values of solvent polarity-polarisability parameter and numbers are listed in Table 1.

Because, the amplitude of the ns-component in the emission decay is only 1–3%, we used the apparent global quantum yield Φ_f and τ_1 for calculating k_r and k_{nr} values (Table 2). The values of k_{nr} are in the range of (15–40) $\times 10^9\ s^{-1}$ except for EG and DMSO (from Sigma–Aldrich, Anhydrous, ≥99.9%). The difference reflects the high viscosity and polarity of these two media. We note also that while the values of k_r are in the range of (1–2) $\times 10^8\ s^{-1}$, in DMSO ($5 \times 10^8\ s^{-1}$) is larger. This suggests that when compared to the result in other media, the emitting state in DMSO (a very large polar and basic solvent) might experience significant different relaxations from those occurring in the other media. As we previously suggested, two close-lying singlet (n,π^*) and (π,π^*) electronic states might be present due to pyridyl and pyridone moieties, and the vibronic coupling between them could be significantly affected by this solvent, and by the no-planarity of MIR. For 1-methyl-2(1H)-pyridinimine (n,π^*) states between the first (π,π^*) and the second (π,π^*) singlet excited sates have been found close lying to the $S_1(\pi,\pi^*)$ state [32]. The low emission quantum yield was explained in terms of no planarity of the structure at S_1 and mixing between (n,π^*) and (π,π^*) states. For 2-PY, two close-in-energy structures have been found in a cold molecular beam expansion, and assigned to conformers of different planarity of the ring [30]. Both situations may happen in MIR, and would partly contribute to its fast photophysics in solution. In rigid media (polymeric matrix) or within a caging nanocavity, the emission quantum yield significantly increases, due to a restriction of molecular motion in the non-radiative decay of MIR [4,15].

To gain further insight into the solvent effect on the fast relaxation of MIR, we analyzed the k_{nr} values with different solvent parameters. To begin with $f(\varepsilon,n)$, the results show that, there is no good correlation between k_{nr} and this parameter. We have observed no correlation using E_T (30) scale. However, k_{nr} variation was correlated with π^* scale (Fig. 4).

Furthermore, we analyzed the variation of log k_{nr} values using the α, β and π^* scales (Eq. (4)).

$$\log k_{nr} = 11.15 - 0.02\alpha - 0.75\beta - 0.76\pi^*,$$
$$R = 0.658,\quad \text{S.D.} = 0.265 \qquad (4)$$

An improvement of the regression fit is obtained by adding the effect of the viscosity (η) of the medium on k_{nr} (Eq. (5)). As expected the result shows that an increase in η of the medium decreases the value of k_{nr}.

$$\log k_{nr} = 10.67 + 0.03\alpha - 0.51\beta - 0.29\pi^* - 0.44 \log \eta,$$
$$R = 0.992,\quad \text{S.D.} = 0.046 \qquad (5)$$

The effect of acidity is not significant, and if we exclude it from the analysis, we obtain:

$$\log k_{nr} = 10.67 - 0.50\beta - 0.27\pi^* - 0.44 \log \eta,$$
$$R = 0.990,\quad \text{S.D.} = 0.044 \qquad (6)$$

Therefore, the solvent affects the radiationless transitions of K by its basicity, polarity, and viscosity. The negative values of β and π^* coefficients indicate that the non-radiative deactivation processes are favored with decreasing the basicity and the polarity–polarizability of the solvents. Both effects have significant contributions. The small contribution of α suggests that the acidity of the solvent has only weak effect on the non-radiative processes of MIR. It is worth noting that, in Eqs. (2) and (3), α parameter has a significance effect on $\tilde{\nu}_{abs}$ and $\Delta\tilde{\nu}$ values, while a weak one on k_{nr} (Eq. (5)). We explain this interesting behavior in terms of the absence (or weak) of H-bond interactions of MIR at the S_1 state with the solvent. As said above for 2PY complexed to water the H-bond interaction at S_1 is weaker than at S_0, shifting the origin of the 0–0 transition of the complex to the blue side of the absorption spectrum [30]. Femtosecond experiments on MIR using normal and deuterated water show similar emission transients, showing no H/D isotope effect on the H-bonding interaction with water, and therefore suggesting an extremely fast (shorter than 100 fs) intermolecular H-bond interactions of MIR with water [16].

3.3. Viscosity effect on relaxation time of MIR

Fig. 5A shows the effect of solvent viscosity on the UV–vis absorption spectra of MIR using mixtures of water and EG of different compositions. Upon going from water to EG solution, the absorption maximum of the lower energy band is red-shifted from 335 to 345 nm. However, the shape of the spectrum does not change. Fig. 5B depicts the fluorescence emission spectra of MIR in these mixtures. Upon increasing the mole fraction of EG (X_{EG}) in the mixture, the emission intensity increases and a red shift from 385 nm (in water) to 393 nm (in EG) is observed. The inset of Fig. 5B shows the increase of the global emission quantum yield (Φ_f) with X_{EG}. As discussed before, because of the involvement of twisting motion of the pyridone part, the emission characteristics of MIR are expected to be sensitive to the changes in viscosity of the medium. Therefore, Fig. 6A displays representative emission decays of MIR in the used EG–water mixtures, and Table 3 presents the data of the multi-exponential fits and Φ_f together with the radiative (k_r) and non-radiative (k_{nr}) rate constant values for the different compositions of the mixtures. The increase of Φ_f and therefore the decrease of k_{nr} upon increasing viscosity of the medium clearly indicate that the twist-

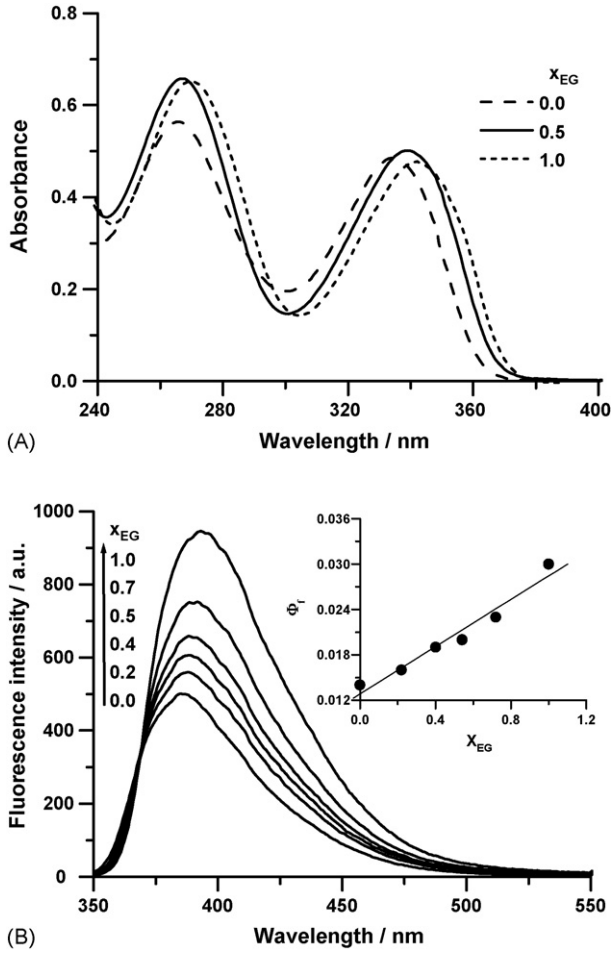

Fig. 5. (A) UV–vis absorption and (B) emission spectra of MIR in water–EG mixtures of different X_{EG} values. The inset of (B) shows the variation of fluorescence quantum yield (Φ_f) vs. X_{EG} upon excitation at 340 nm.

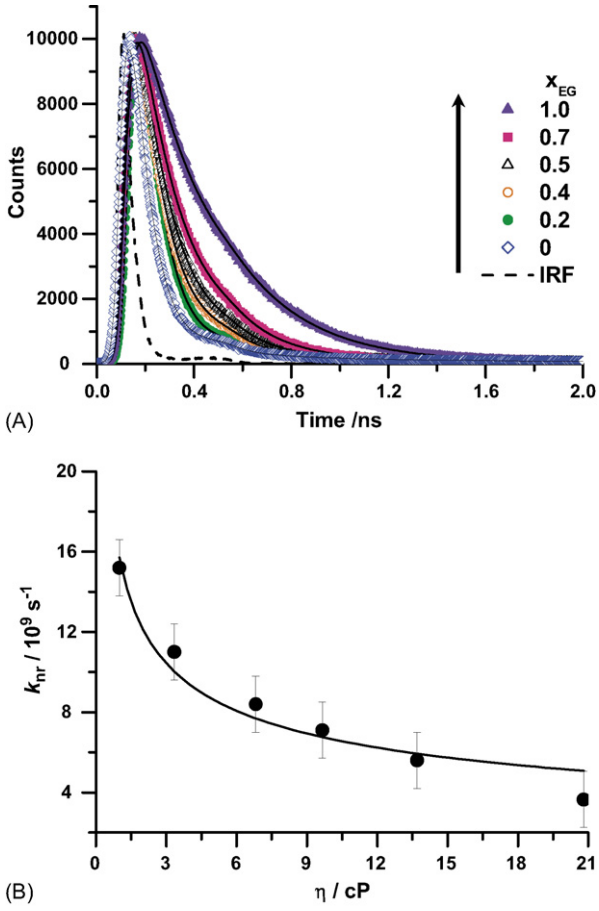

Fig. 6. (A) Emission decays of MIR in water–EG mixtures of different X_{EG} values gated at 440 nm. The data of the multi-exponential fits (solid lines) are shown in Table 2. (B) Variation of non-radiative rate constant (k_{nr}) of MIR with viscosity (η) of water–EG mixtures.

ing motion of the pyridone moiety, and probably that of methyl group rotation affecting the molecular planarity are one of the main efficient radiationless channels. Because of the H-bonding ability and polarity of the water–EG mixtures do not change significantly with the molar fraction of water, the observed change in k_{nr} is mainly due to viscosity variation. Comparing with other drugs, piroxicam showed high sensitivity towards solvent polarity [33]. As previously said, the coupling between $S_1(\pi,\pi^*)$ and $S_2(n,\pi^*)$ states should be enhanced by any change in the coplanarity of the molecular frame of the molecule, including those provoked by the methyl and pyridyl ring rotations. Thus, in addition to the polarity effect in the vibronic coupling, an increase in the viscosity of the used EG–water mixtures will decrease molecular distortion and therefore reduces the vibronic coupling and the non-radiative rate constant value.

Fig. 6B displays a plot of k_{nr} versus the viscosity (η) values of the used mixtures [34]. The experimental data were analyzed following the expression [35]:

$$k_{nr} = \left(\frac{C}{\eta^m}\right) \exp\left(-\frac{E_0}{RT}\right) \quad (7)$$

where C is a constant, $0 \leq m \leq 1.0$ and E_0 is the activation energy of the non-radiative processes. To extract the values of these parameters, we wrote Eq. (7) in the form $k_{nr} = A/\eta^m$, where

Table 3
Photophysical emission decay parameters of MIR in water–ethylene glycol mixtures

X_{EG}	η (cP)	τ_1 (ps)	a_1 (%)	τ_2 (ns)	a_2 (%)	Φ_f	k_r (10^8 s^{-1})	k_{nr} (10^9 s^{-1})
0	1.0	65	99	1.34	1	0.014	2.1 ± 0.4	15 ± 3
0.22	3.33	89	99	1.15	1	0.016	1.8 ± 0.4	11 ± 3
0.40	6.82	116	99	1.12	1	0.019	1.6 ± 0.4	8.4 ± 2
0.54	9.65	138	98	1.04	2	0.020	1.5 ± 0.3	7.1 ± 2
0.72	13.70	173	99	1.06	1	0.023	1.3 ± 0.3	5.6 ± 1
1.00	20.80	270	99	1.09	1	0.030	1.1 ± 0.3	3.6 ± 1

X_{EG} is the mole fraction of ethylene glycol. This table gives the viscosity of the media.

A is a constant. A linear correlation between $\ln k_{nr}$ and $\ln \eta$ gives $m \approx 0.4$ and $A = 1.7 \times 10^{10}\ s^{-1}$. Values for $m = 0.23$–1.0, and $C = 1 \times 10^{10}$ to $4 \times 10^{12}\ s^{-1}$ have been reported [35–39]. Note that the obtained value for $m \approx 0.4$ (in Eq. (7)) is similar (0.44) to that obtained for the coefficient of $\log \eta$ in Eqs. (5) and (6) which examine the effect of other solvent parameters in addition to the viscosity one. Thus, for $m \approx 0.4$ and when $C \approx 4 \times 10^{12}\ s^{-1}$ we obtain $E_0 = 3.2$ kcal/mol ($R^2 = 0.967$), and when $C = 1 \times 10^{10}\ s^{-1}$ we found $E_0 = 1.1$ kcal/mol. The values of E_0 are comparable to those found (1–4 kcal/mol) for molecules undergoing photoinduced conformational changes and showing dynamical solvent effects [35–39].

3.4. Viscosity effect on rotational time of MIR

To gain information on the rotational times (ϕ) of MIR and therefore on its interaction with the solvation shell, we have performed time-resolved emission anisotropy measurements in water–EG mixtures. Fig. 7A shows representative $r(t)$ decays. These do not show a significant change when measuring at different wavelengths of observation over the emission band. The decays fit to a single-exponential function. The obtained ϕ values increase from 67 ± 15 ps in pure water to 568 ± 60 ps in pure EG (Table 4). Clearly and as it is expected from the hydrodynamic theory [40,41], the rotational motion of the drug is slower in more viscous mixtures.

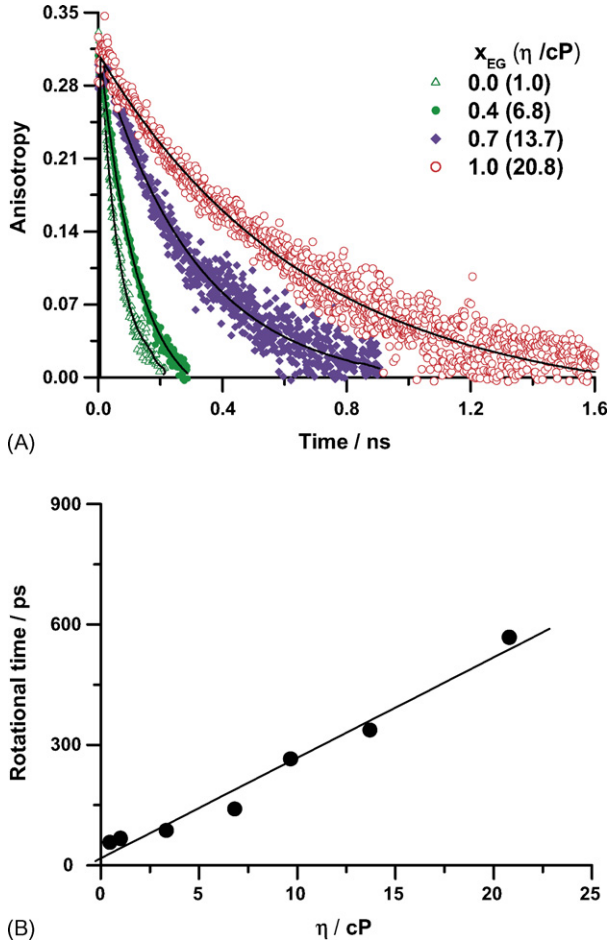

Fig. 7. (A) Anisotropy decays of MIR in water–EG mixtures of different X_{EG} values, gated at 440 nm. (B) Variation of rotational time (ϕ) of MIR with the viscosity (η) of water–EG mixtures. The solid curve is a fit supposing a linear change of ϕ with η.

Table 4
Rotational time values (ϕ) of MIR in water–EG mixtures of different X_{EG} and viscosity values

X_{EG}	ϕ (ps)	η (cP)[a]
0	67 ± 15	1.0
0.22	88 ± 18	3.34
0.40	140 ± 25	6.82
0.54	265 ± 40	9.65
0.72	337 ± 50	13.7
1.00	568 ± 60	20.8

The gating emission was 440 nm. The viscosity values are from Ref. [35].
[a] Viscosity at 293 K [34].

Fig. 7B shows a linear correlation between the rotational time and the viscosity of the solvent mixtures [34]. This result indicates that the viscosity is the main factor that determines the rotational relaxation time of MIR in these mixtures. The fit of the data yields a correlation coefficient of 0.987, with a slope of 25 ± 3 ps/cP and an intercept of ~16 ps at $\eta = 0$. Similar nonzero intercept has been observed previously in other compounds [42–44]. However, there is no clear physical meaning to explain its value at $\eta = 0$ [43].

We used the anisotropy data to get information on the hydrodynamic behavior of MIR. Geometry optimization of MIR shows that MIR has an ellipsoid shape with semimajor axis values $b = 3.5$ Å and $a = c = 4.65$ Å, and a volume ($V = 4\pi abc/3$) $V = 229$ Å^3. According to the Stokes–Einstein–Debye hydrodynamic theory [40,41], the rotational time (ϕ) of a rotor is related to V by

$$\phi = \frac{\eta V(fC)}{k_B T} \tag{8}$$

where η is the viscosity of the solvent, k_B the Boltzmann constant, T the absolute temperature and f is a shape factor of the solute ($f = 1$ for a sphere). For non-spherical molecules, $f > 1$ and the magnitude of the deviation from unity in the value of f describes the degree of the non-spherical nature of the solute rotor. The value of f was determined from the molecular dimensions as 1.1 and 0.055 under stick and slip boundary conditions, respectively [44]. The coupling parameter C is depending on the boundary condition. The two limiting cases are the hydrodynamic stick and slip. For a non-spherical solute molecule, the value of C is a sensitive function of solute shape and it is in the range $0 < C \leq 1$. Its magnitude depends on solute–solvent friction and on the relative size of the solute compared to that of solvent molecules. From the slope of Fig. 7B (25 ps/cP) and using Eq. (8), we calculated under stick- and slip-boundary condition limits, the value of C, and we got 0.4 and 8, respectively. Whereas the slip prediction is out of the limiting range of C ($0 < C \leq 1$), the stick one seems reasonable. We conclude that the excited MIR is rotating under stick condition in the used water–EG mixtures. Therefore, a solvation shell involving water or/and EG molecules is rotating with MIR. It has been observed

that the value of C decreases as the relative solvent/solute size ratio increases [42]. C values of 0.11–0.78 were observed for coumarin 153, with comparable size to MIR, in different solvents [42].

Finally, the initial value of $r(t)$ in these media is ∼0.32, not very different from the ideal one (0.4), indicating that the emission transition moment of MIR has rotated by ∼21° to that of its absorption.

4. Conclusion

The present study shows the role of specific interactions between different sites of MIR and solvent molecules. In strongly polar solvents, a possible vibronic coupling of $S_1(\pi,\pi^*)$ with a close lying $S_2(n,\pi^*)$ state should decrease, and therefore leads to a slowing of non-radiative rate constants when compared to those found in nonpolar solvents. In addition to that, molecular distortion and twisting motion of the pyridyl part, which enhance radiationless transitions and vibronic coupling, are slowed in highly viscous solvents. Because of the H-bond donating and accepting sites of MIR, the effect of H-bond donor and acceptor solvent shows reversed trends. Furthermore, the solvent effect on the dynamical behavior (k_{nr}) indicates a decrease of H-bond interaction of accepting groups of MIR with the media, most probably due to a fast ICT reaction. Time-resolved ps-emission anisotropy experiments combined with theory suggests that the interaction of MIR in the used mixtures of EG and water is strong enough that the solvation shell is rotating with the drug.

Acknowledgements

This work was supported by the "Consejeria de Sanidad" of JCCM and MEC through projects SAN-04-000-00 and SAB2004-0086. M.E. thanks the MEC for the sabbatical year fellowship.

References

[1] A. Alousi, J. Canter, M. Montenaro, D. Fort, R. Ferrari, J. Cardiovasc. Pharmacol. 5 (1983) 792.
[2] C. Altomare, S. Cellamare, L. Summo, P. Fossa, L. Mosti, A. Carotti, Bioorg. Med. Chem. 8 (2000) 909.
[3] M. de Candia, P. Fossa, S. Cellamare, K. Mosti, A. Carotti, C. Altomare, Eur. J. Pharm. Sci. 26 (2005) 78.
[4] M. El-Kemary, J.A. Organero, A. Douhal, J. Med. Chem. 49 (2006) 3086.
[5] M. Karelson, A.R. Katritzky, M. Szafran, M. Zerner, J. Org. Chem. 54 (1989) 6030.
[6] A. Cordon, A.R. Katritzky, S.K. Roy, J. Chem. Soc. B (1968) 556.
[7] A. Krauze, R. Vĭtolina, V. Garaliene, L. Sĭle, V. Kluša, G. Duburs, Eur. J. Med. Chem. 40 (2005) 1163.
[8] J. Bayliss, M. Norell, R. Canepa-Anson, S.R. Reuban, P.A. Poole-Wilsn, G.C. Sutton, Br. Heart J. 49 (1983) 214.
[9] S.J. Siskind, E.H. Sonnenblick, R. Forman, J. Scheuer, T.H. LeJemtel, Circulation 64 (1981) 966.
[10] J.R. Benotti, W. Grossman, E. Braunwald, B.A. Carabello, Circulation 62 (1980) 28.
[11] K.T. Weber, V. Andrews, J.S. Janicki, J.R. Wilson, A.P. Fishman, Am. J. Cardiol. 48 (1981) 164.
[12] S. Monti, S. Sortino, Chem. Soc. Rev. 31 (2002) 287.
[13] H.-R. Park, T.H. Kim, K.-M. Bark, Eur. J. Med. Chem. 37 (2002) 443.
[14] M. El-Kemary, A. Douhal, in: A. Douhal (Ed.), Cyclodextrin Materials Photochemistry, Photophysics and Photobiology, Elsevier, 2006 (Chapter 4).
[15] M. El-Kemary, J.A. Organero, L. Santos, A. Douhal, J. Phys. Chem. B 110 (2006) 14128.
[16] M. Gil, A. Douhal, Chem. Phys. Lett. 428 (2006) 174.
[17] D.F. Eaton, Pure Appl. Chem. 60 (1988) 1107.
[18] J.A. Organero, L. Tormo, A. Douhal, Chem. Phys. Lett. 263 (2002) 409.
[19] V. Barone, C. Adamo, J. Photochem. Photobiol. A: Chem. 80 (1994) 211.
[20] M. Terazima, T. Azumi, J. Am. Chem. Soc. 111 (1989) 3824.
[21] J. Sepiol, H. Bulska, A. Grabowska, Chem. Phys. Lett. 140 (1987) 607.
[22] M. El-Kemary, M. El-Khouly, O. Ito, Photochem. Photobiol. A: Chem. 137 (2000) 105.
[23] D.W. Robertson, E.E. Beedle, J.K. Swartzendruber, N.D. Jones, T.K. Elzey, R.F. Kauffman, H. Wilson, J.S. Hayes, J. Med. Chem. 29 (1986) 635.
[24] C. Reichardt, Chem. Rev. 94 (1994) 2319.
[25] J.-L.M. Abboud, R. Notario, Pure Appl. Chem. 71 (1999) 645, and references therein.
[26] M.L. Horng, J.A. Gardecki, A. Papazyan, M. Maroncelli, J. Phys. Chem. 99 (1995) 17311.
[27] G. Wenska, B. Skalski, Z. Gdaniec, R.W. Adamiak, J. Matulic-Adamic, L. Beigelman, J. Photochem. Photobiol. A: Chem. 133 (2000) 169.
[28] P. Pradhan, B. Singh, C. Nandi, T. Chakraborty, T. Kundu, J. Chem. Phys. 122 (2005) 1.
[29] G.N. Patwari, T. Ebata, N. Mikami, J. Phys. Chem. A 105 (2001) 8642.
[30] M.R. Nimlos, D.F. Kelley, E.R. Bernstein, J. Phys. Chem. 93 (1989) 643.
[31] A. Testa, J. Photochem. Photobiol. A: Chem. 64 (1992) 73.
[32] K. Inuzuka, N. Iwaski, A. Fujimoto, Chem. Soc. Jpn. Chem. Ind. Chem. J. 7 (2001) 2001.
[33] S.M. Andrade, S.M.B. Costa, Phys. Chem. Chem. Phys. 1 (1999) 4213.
[34] N.G. Tsierkezos, I.E. Molinou, J. Chem. Eng. Data 43 (1998) 989.
[35] S.H. Courtney, G.R. Fleming, J. Chem. Phys. 83 (1985) 215.
[36] G.C. Kelly, E.L. Quitevis, J. Phys. Chem. 92 (1988) 6590.
[37] K. Das, D.S. English, J.W. Petrich, J. Am. Chem. Soc. 119 (1997) 2793.
[38] F.E. Doany, E.J. Heilweil, R. Moore, R. Hochstrasser, J. Chem. Phys. 80 (1984) 201.
[39] C.J. Tredwell, A.D. Osborne, J. Chem. Soc., Faraday Trans. II 76 (1980) 1627.
[40] F. Perrin, J. Phys. Radium 5 (1934) 497.
[41] C.-M. Hu, R. Zwanzig, J. Chem. Phys. 60 (1974) 4354.
[42] M.-L. Horng, J.A. Gardecki, M. Maroncelli, J. Phys. Chem. A 101 (1997) 1030.
[43] G. Burdzinski, G. Buntinx, O. Poizat, P. Toele, H. Zhang, M. Glasbeek, Chem. Phys. Lett. 392 (2004) 470.
[44] R.M. Anderton, J.F. Kauffman, J. Phys. Chem. 98 (1994) 12117.